Dark energy-like stars from nonminimally coupled scalar field



2013 Class. Quantum Grav. 30 145006

(http://iopscience.iop.org/0264-9381/30/14/145006)

Class. Quantum Grav. **30** (2013) 145006 (19pp) doi:10.1088/0264-9381/30/14/145006

# Dark energy-like stars from nonminimally coupled scalar field

**Dubravko Horvat and Anja Marunović**

University of Zagreb, Faculty of Electrical Engineering and Computing, Physics Department, Unska 3, 10000 Zagreb, Croatia

E-mail: dubravko.horvat@fer.hr and anja.marunovic@fer.hr

Received 25 January 2013, in final form 22 May 2013
Published 12 June 2013
Online at stacks.iop.org/CQG/30/145006

**Abstract**

We show that even a rather *minimal* extension of the Einstein–Hilbert action by a nonminimal coupling of the scalar field to the Ricci curvature scalar results in configurations that resemble more the dark energy stars than the ordinary boson stars. Even though many of those configurations are endowed by negative principal pressures, the strong energy condition, as a signal of repulsive gravity, is not significantly violated in these configurations. When imposing restrictions on matter from energy conditions we find that the maximally allowed masses are shifted to the lower values due to the violation of the weak and dominant energy conditions. We also calculate the effective compactness and show that its maximum value is attained in the region of negative pressures, and is greater than that in ordinary boson stars. Moreover, we develop a universality technique which allows us to efficiently map small configurations that are easily solved by numerical methods, to large astrophysical objects.

PACS numbers: 04.20−q, 04.25.D−, 04.40.−b, 04.50.Kd, 95.30.Sf, 98.80.Jk

(Some figures may appear in colour only in the online journal)

## 1. Introduction

One of the most peculiar predictions of classical general relativity, at least if matter obeys the strong energy condition (SEC) are black holes. (According to the SEC the sum of the energy density and pressures, $\rho + \sum p_i \geqslant 0$, cannot be negative.) When quantum effects are included, black holes lead to a number of thermodynamic paradoxes associated with Hawking radiation and the implied information loss in black hole spacetimes, thus questioning whether the final stage of a massive star collapse is a black hole, or perhaps some other as-yet-not-understood dense object that stops a further collapse. Sakharov was the first who introduced the concept of nonsingular collapse through the equation of state (EoS) for the cosmological dark energy (for which $p \simeq -\rho$) as a super-dense fluid [1] and then Gliner assumed that such a fluid could

  

be the final state of gravitational collapse [2]. Inspired by these ideas, Mazur and Mottola investigated alternative configurations which led to a solution dubbed gravastar (*gra*vitational *va*cuum *star*) [3]. This anisotropic, highly compact astrophysical object consists of a de Sitter core and through a vacuum phase transition layer matches an exterior Schwarzschild spacetime by avoiding an event horizon formation. Although gravastar configurations rest upon a very attractive idea, all these models are macroscopic in the sense that their foundation rest on studying Einstein's theory in the presence of a matter fluid that obeys some phenomenological EoS, and as such do not have a proper field-theoretic foundation. Both cases—when the energy density is distributed on thin-shells (see e.g. [4, 5]) and when it continuously varies throughout the star [6–8]—rely on the so-called *Ansätze*-approach. In this approach, Einstein's equations are solved in the presence of a radially distributed matter fluid, for which an EoS or some other relation among the thermodynamic functions (the energy density, the radial and tangential pressures) is provided. All these models are essentially toy models, and they are important in the sense that they can be used to provide a better understanding of the main characteristics of black hole mimickers. But a complete understanding of these objects will be attained only if we can provide their faithful microscopic (field-theoretic) models.

Apart from a better understanding at the fundamental level, field-theoretic models of highly compact nonsingular objects, obtained from a suitable lagrangian of interacting matter fields, can provide a fundamental explanation for the anisotropy in the principal pressures, which occurs naturally in the stars made of scalar fields, the so-called boson stars. Boson stars are nonsingular asymptotically flat solutions of the Einstein–Klein–Gordon field equations which govern massive complex scalar fields coupled to gravity. The extensive research was started by Kaup [9], who has introduced the notion of the gravitationally bound state of scalar particles. Soon many papers considering various versions of scalar field configurations appeared [10–15]. The growing importance of boson stars resulted in extensive research which has been reviewed in [16–19]. When the boson star configurations are considered, one immediately recognizes that a massive scalar field, even if self-interacting, cannot produce anisotropy which could support an object with (asymptotically) de Sitter interior. Albeit boson stars belong to the realm of very compact objects; it turns out that getting closer to the main black hole features requires modification of general relativity. Even though Einstein's theory has passed all observational tests in the weak field limit, the *true* theory of gravity may differ significantly in the regime of strong gravitational fields. Moreover, large-scale cosmological observations and conceptual difficulties in quantizing general relativity call for its modifications.

In this paper, we show that even a rather *minimal* extension of the Einstein–Hilbert action by a nonminimal coupling of the scalar field to the Ricci curvature scalar results in configurations that resemble more the dark energy stars than the ordinary boson stars. Even though many of those configurations are endowed by negative principal pressures, the SEC, as a signal of repulsive gravity, is not significantly violated in these configurations. Yet, the maximum effective compactness is attained in the region of negative pressures, and is greater than that in ordinary boson stars. This fact supports an idea that the dark energy stars might present a promising black hole mimicker. While some attempts have been made to study dark energy stars (see for example [20–25]), which are loosely speaking in the literature taken as objects that contain a negative pressure somewhere in the interior, no systematic study has been so far performed of whether and when boson stars in nonminimal setting violate energy conditions. In this work we fill that gap.

The paper is organized as follows. In section 2, we present the basic Einstein equations for spherically symmetric configurations of a nonminimally coupled complex scalar field. In section 3, a brief description of ordinary boson star solutions is presented which leads to a situation in which a necessity of additions mechanism is needed. The nonminimal coupling

is introduced in section 4, where we present solutions with required anisotropic behaviour of pressures, i.e. dark energy-like stars comprising negative pressures. In that section, we also perform analysis of the parameter space for which the weak and dominant energy conditions are violated. Moreover, we investigate the effective compactness. Finally, in section 5, we discuss our results and give an outlook for future work.

## 2. Theory behind—equilibrium configurations

For gravity, we take the standard Einstein–Hilbert action

$$S_{\mathrm{EH}} = \int \mathrm{d}^4x\sqrt{-g}\frac{R}{16\pi G_N}, \tag{1}$$

where $G_N$ is the Newton constant, $R$ is the Ricci scalar and $g$ is the determinant of the metric tensor $g_{\mu\nu}$, which is given by

$$g_{\mu\nu} = \mathrm{diag}(-\mathrm{e}^{\nu(r)}, \mathrm{e}^{\lambda(r)}, r^2, r^2\sin^2\theta). \tag{2}$$

The spacetime metric is static and spherically symmetric as we are interested only in spherically symmetric equilibrium configurations. For matter, we take an action of a complex scalar field with a mass $m_\phi$ and a quartic self-interaction $\lambda_\phi$ coupled nonminimally to gravity:

$$S_\phi = \int \mathrm{d}^4x\sqrt{-g}\left(-g^{\mu\nu}\partial_\mu\phi^*\partial_\nu\phi - m_\phi^2\phi^*\phi - \frac{\lambda_\phi}{2}(\phi^*\phi)^2 + \xi R\phi^*\phi\right), \tag{3}$$

where $\xi$ measures the strength of the coupling between the scalar field $\phi$ and gravity *via* the Ricci scalar $R$ and $\phi^*$ is the complex conjugate of $\phi$. It is worth noting here that in order to produce stable configurations, the scalar field must be complex. According to the *Derrick theorem* [26], regular, static, nontopological, localized scalar field solutions cannot be created by real scalar fields (see [27] and e.g. [16]).

The energy–momentum tensor of a complex scalar field is obtained by varying its action with respect to the metric tensor $g^{\mu\nu}$:

$$\begin{aligned} T^\phi_{\mu\nu} = {} & 2\delta^\alpha_{(\mu}\delta^\beta_{\nu)}\partial_\alpha\phi^*\partial_\beta\phi - g_{\mu\nu}\left[g^{\alpha\beta}\partial_\alpha\phi^*\partial_\beta\phi + m_\phi^2\phi^*\phi + \tfrac{1}{2}\lambda_\phi(\phi^*\phi)^2\right] \\ & - 2\xi\phi^*\phi G_{\mu\nu} + 2\xi\nabla_\mu\nabla_\nu(\phi^*\phi) - 2\xi g_{\mu\nu}\Box(\phi^*\phi). \end{aligned} \tag{4}$$

By varying now the full action

$$S = S_{\mathrm{EH}} + S_\phi \tag{5}$$

with respect to the metric tensor $g^{\mu\nu}$, we obtain the Einstein equations

$$R_{\mu\nu} - \tfrac{1}{2}g_{\mu\nu}R = 8\pi G_N T_{\mu\nu}. \tag{6}$$

The Klein–Gordon equation, the equation of motion for the scalar field $\phi$ (or $\phi^*$), is obtained from Bianchi identities or by varying (5) with respect to $\phi^*$ (or $\phi$), resulting in

$$\left[\Box - m_\phi^2 - \lambda_\phi\phi^*\phi + \xi R\right]\phi = 0. \tag{7}$$

In order to proceed, we choose a harmonic time dependence for the scalar field

$$\phi(r,t) = \phi_0(r)\,\mathrm{e}^{-\imath\omega t}, \qquad \phi_0(r) \in \mathbb{R}. \tag{8}$$

Even though the scalar field that induces the metric is time dependent, the energy–momentum tensor created by this field is time independent and thus leads to time-independent metric functions. Hence, condition (8) does not contradict the Birkhoff theorem. Furthermore, the same *Ansatz* for the classical field was also used in [28] bearing the name *coherent*

*state*, presumably alluding to their resemblance to quantum coherent states[1]. Highly excited field configurations were used to explain flat rotation curves inside galactic halos in [29]. Furthermore, in [30] it was shown that it is possible to construct a stable multistate boson star, with coexisting ground and first excited states.

Upon inserting the Ansätze (8) and (2) into (4) one obtains for non-vanishing components of the stres–energy tensor:

$$T_t^t = \left(-m_\phi^2 - \omega^2 \mathrm{e}^{-\nu} - \frac{\lambda_\phi}{2}\phi_0^2\right)\phi_0^2 - \mathrm{e}^{-\lambda}(1+4\xi)\phi_0'^2 - 2\xi\phi_0^2 G_t^t \\ - 4\xi \mathrm{e}^{-\lambda}\left[\phi_0'' + \left(\frac{\nu'-\lambda'}{2} + \frac{2}{r}\right)\phi_0'\right]\phi_0 + 2\xi \mathrm{e}^{-\lambda}\nu'\phi_0\phi_0' \tag{9}$$

$$T_r^r = \left(-m_\phi^2 + \omega^2 \mathrm{e}^{-\nu} - \frac{\lambda_\phi}{2}\phi_0^2\right)\phi_0^2 + \mathrm{e}^{-\lambda}\phi_0'^2 - 2\xi\phi_0^2 G_r^r - 2\xi \mathrm{e}^{-\lambda}\left(\nu' + \frac{4}{r}\right)\phi_0\phi_0', \tag{10}$$

$$T_\theta^\theta = \left(-m_\phi^2 + \omega^2 \mathrm{e}^{-\nu} - \frac{\lambda_\phi}{2}\phi_0^2\right)\phi_0^2 - \mathrm{e}^{-\lambda}\phi_0'^2 - 2\xi\phi_0^2 G_\theta^\theta \\ - 4\xi \mathrm{e}^{-\lambda}\left[\phi_0'' + \left(\frac{\nu'-\lambda'}{2} + \frac{2}{r}\right)\phi_0'\right]\phi_0 - 4\xi\frac{\mathrm{e}^{-\lambda}}{r}\phi_0\phi_0', \tag{11}$$

$$T_\phi^\phi = T_\theta^\theta. \tag{12}$$

Similarly, the scalar field equation of motion (7) becomes

$$\phi_0'' + \left(\frac{2}{r} + \frac{\nu'-\lambda'}{2}\right)\phi_0' - \mathrm{e}^{\lambda}\left(m_\phi^2 + \lambda_\phi\phi_0^2 - \omega^2\mathrm{e}^{-\nu} - \xi R\right)\phi_0 = 0. \tag{13}$$

By virtue of (13) it is possible to eliminate the second derivative of the scalar field $\phi_0''$ in the components of the energy–momentum tensor (9)–(12), leading to the following form for the first two Einstein equations ($G_\mu^\nu = 8\pi G_N T_\mu^\nu$):

$$\left[1 + 2\xi(8\pi G_N)\phi_0^2\right]G_t^t = 8\pi G_N\left\{\left(-m_\phi^2 - \omega^2\mathrm{e}^{-\nu} - \frac{\lambda_\phi}{2}\phi_0^2\right)\phi_0^2 - \mathrm{e}^{-\lambda}(1+4\xi)\phi_0'^2 \right. \\ \left. - 4\xi\left[m_\phi^2 + \lambda_\phi\phi_0^2 - \omega^2\mathrm{e}^{-\nu} - \xi R\right]\phi_0^2 + 2\xi\mathrm{e}^{-\lambda}\nu'\phi_0\phi_0'\right\}, \tag{14}$$

$$\left[1 + 2\xi(8\pi G_N)\phi_0^2\right]G_r^r = 8\pi G_N\left\{\left(-m_\phi^2 + \omega^2\mathrm{e}^{-\nu} - \frac{\lambda_\phi}{2}\phi_0^2\right)\phi_0^2 \right. \\ \left. + \mathrm{e}^{-\lambda}\phi_0'^2 - 2\xi\mathrm{e}^{-\lambda}\left(\nu' + \frac{4}{r}\right)\phi_0\phi_0'\right\}, \tag{15}$$

where

$$G_t^t = -\mathrm{e}^{-\lambda}\left(\frac{\lambda'}{r} + \frac{\mathrm{e}^{\lambda}}{r^2} - \frac{1}{r^2}\right), \tag{16}$$

$$G_r^r = \mathrm{e}^{-\lambda}\left(\frac{\nu'}{r} - \frac{\mathrm{e}^{\lambda}}{r^2} + \frac{1}{r^2}\right). \tag{17}$$

[1] One should keep in mind however that a scalar field written as in (8), apart from the ground state, can also represent excited states with higher energy, and a particular combination of these states can indeed form coherent states. In general, these states contain 'coherent' radial oscillations, but do not in the usual sense constitute quantum coherent states.

There is one more independent equation. Instead of using the $(\theta\theta)$ Einstein equation (or the equivalent $(\varphi\varphi)$ equation), it is in fact more convenient to use the trace equation, $G^{\mu}_{\mu} = -R = 8\pi G_N T^{\mu}_{\mu}$, leading to

$$R = \frac{8\pi G_N\left\{2m_\phi^2\phi_0^2 + 2(1+6\xi)\left[\mathrm{e}^{-\lambda}\phi_0'^2 + (m_\phi^2 - \omega^2\mathrm{e}^{-\nu} + \lambda_\phi\phi_0^2)\right]\phi_0^2\right\}}{1 + 2\xi(1+6\xi)8\pi G_N\phi_0^2}. \tag{18}$$

It is instructive to add a couple of remarks on this equation. For the case of conformal coupling, $\xi = -1/6$, the only non-vanishing term in the Ricci curvature scalar is the scalar field mass. Hence, in limit of a vanishing scalar field mass, for which the Ricci scalar is zero, one obtains a conformal gravity limit, as expected. Nevertheless, for $\xi \neq -1/6$, as we shall see in the subsequent sections, a variety of configurations is possible.

Equations (14)–(15) and (18) constitute the central equations in this work.

### *2.1. Dimensionless variables*

Before we proceed to solving equations (14)–(15) and (18), for the purpose of numerical studies, it is convenient to work with dimensionless variables/functions. To this purpose, we perform the following rescalings:

$$\begin{aligned} &\frac{r}{\sqrt{8\pi G_N}} \to x, \qquad 8\pi G_N\phi_0(r)^2 \to \sigma(r)^2, \\ &8\pi G_N R \to \tilde{R}, \qquad 8\pi G_N m_\phi^2 \to \tilde{m}_\phi^2, \qquad 8\pi G_N\omega^2 \to \tilde{\omega}^2. \end{aligned} \tag{19}$$

Upon these transformations, all variables/functions get expressed in terms of reduced Planck units:

$$\begin{aligned} &\bar{m}_P = m_P/\sqrt{8\pi}, \quad \text{with the Planck mass} \quad m_P = \sqrt{\frac{\hbar c}{G_N}} = 1.2209\times 10^{19}\mathrm{GeV}/c^2 \\ &\qquad\qquad\qquad\qquad\qquad\qquad\qquad\qquad\qquad\qquad = 2.17651(13)\times 10^{-8}\mathrm{kg}, \\ &\bar{l}_P = \sqrt{8\pi}\,l_P, \quad \text{with the Planck length} \quad l_P = \sqrt{\frac{\hbar G_N}{c^3}} = 1.616199(97)\times 10^{-35}\mathrm{m}. \end{aligned} \tag{20}$$

The rescaled (dimensionless) differential equations to be solved are then

$$\begin{aligned} \lambda' = \frac{1-\mathrm{e}^{\lambda}}{x} + x\frac{\mathrm{e}^{\lambda}\left(\tilde{m}_\phi^2 + \tilde{\omega}^2\mathrm{e}^{-\nu} + \frac{\lambda_\phi}{2}\sigma^2\right)\sigma^2 + (1+4\xi)\sigma'^2 - 2\xi\nu'\sigma\sigma'}{1+2\xi\sigma^2} \\ + \frac{4x\xi\mathrm{e}^{\lambda}\left(\tilde{m}_\phi^2 - \tilde{\omega}^2\mathrm{e}^{-\nu} + \lambda_\phi\sigma^2 - \xi\tilde{R}\right)\sigma^2}{1+2\xi\sigma^2}, \end{aligned} \tag{21}$$

$$\nu' = \frac{(\mathrm{e}^{\lambda}-1)(1+2\xi\sigma^2)/x + x\mathrm{e}^{\lambda}\left(-\tilde{m}_\phi^2 + \tilde{\omega}^2\mathrm{e}^{-\nu} - \frac{\lambda_\phi}{2}\sigma^2\right)\sigma^2 + x\sigma'^2 - 8\xi\sigma\sigma'}{1+2\xi\sigma^2+2\xi x\sigma\sigma'}, \tag{22}$$

$$\sigma'' = -\left(\frac{2}{x} + \frac{\nu'-\lambda'}{2}\right)\sigma' + \mathrm{e}^{\lambda}\left(\tilde{m}_\phi^2 + \lambda_\phi\sigma^2 - \tilde{\omega}^2\mathrm{e}^{-\nu} - \xi\tilde{R}\right)\sigma, \tag{23}$$

with the dimensionless Ricci scalar

$$\tilde{R} = \frac{2\tilde{m_\phi}^2\sigma^2 + 2(1+6\xi)\left[\left(\tilde{m}_\phi^2 - \tilde{\omega}^2\mathrm{e}^{-\nu} + \lambda_\phi\sigma^2\right)\sigma^2 + \mathrm{e}^{-\lambda}\sigma'^2\right]}{1+2\xi(1+6\xi)\sigma^2}, \tag{24}$$

where now the *primes* denote derivatives with respect to $x$.

Equations (21)–(23) yield a unique solution (that depends of course on $\sigma_0$) when subject to the boundary conditions:

$$(1)\quad \lambda(0)=0, \qquad (2)\quad \nu(\infty)=0, \qquad (3)\quad \sigma(0)=\sigma_0, \qquad (4)\quad \sigma(\infty)=0. \tag{25}$$

The first boundary condition ensures that the *mass function* $m(r)$ defined in terms of the metric function as

$$\mathrm{e}^{-\lambda}=1-\frac{2G_N m(r)}{r}=1-\frac{2\tilde{m}(x)}{x} \tag{26}$$

is zero at $r=0$ (or equivalently at $x=0$). The second boundary condition in (25) ensures asymptotic flatness at large distances,

$$\mathrm{e}^{\nu(r)}|_{r\to\infty}=\left(1-\frac{2G_N m(r)}{r}\right)\Big|_{r\to\infty}\to 1. \tag{27}$$

The third and fourth boundary conditions in (25) are typical for boson stars with a positive scalar mass term ($m_\phi^2>0$).[2] Equations (21)–(23) together with the boundary conditions (25) constitute an eigenvalue problem for $\omega$, that is, for each central field value $\sigma_0$, there is a unique $\omega$ that satisfies the given boundary conditions. The ground state is characterized by zero nodes in the field $\sigma(x)$ (defined as the points $x$ where $\sigma(x)=0$), while the $n$th excited state has $n$-nodes in $\sigma(x)$. In this paper, if not explicitly stated otherwise, boson stars in their ground state will be studied.

We solve these nonlinear, mutually coupled, differential equations numerically by using the software package *Colsys* [31].

### 2.2. Universality

In order to solve the problem numerically, we need to specify the set of parameters $\{\lambda_\phi, \tilde{m}^2, \tilde{\omega}^2, \xi\}$. However, for a successful numerical integration these parameters cannot be very different from unity. On the other hand, in physically interesting situations these parameters may wildly differ from unity. For example, compact stars have radial size that is measured in kilometres, while numerical solutions give objects whose size is of the order of the Planck length, $l_P\sim 10^{-38}$ km, obviously not very useful. In order to overcome this impasse, we observe that the dimensionless equations (21)–(24) possess a 'conformal' symmetry. Indeed, equations (21)–(24) are invariant under the following conformal transformations:

$$x\to\beta x, \quad \lambda\to\frac{\lambda}{\beta^2}, \quad \tilde{R}\to\frac{\tilde{R}}{\beta^2}, \quad \tilde{m}^2\to\frac{\tilde{m}^2}{\beta^2}, \quad \tilde{\omega}^2\to\frac{\tilde{\omega}^2}{\beta^2}, \quad \sigma\to\sigma, \quad \xi\to\xi. \tag{28}$$

How the mass of the whole boson star changes due to these rescalings can be estimated from the identity

$$M\sim\rho R^3, \tag{29}$$

where $\rho$ is the density which can be approximated by the value of the potential at a scalar field maximum

$$\rho\sim V(\sigma_0)\sim\tilde{m}_\phi^2\sigma_0^2+\lambda_\phi\sigma_0^4. \tag{30}$$

[2] On the other hand, the appropriate boundary conditions in the case of a negative mass term ($m_\phi^2<0$) are $\sigma(0)=0$, $\sigma(\infty)=\sigma_0$, resulting in topologically stable configurations known as *global strings*. More generally, a multicomponent scalar field with appropriate boundary conditions can generate global topological defects which have been extensively studied in cosmology.

On the other hand, from the virial theorem, according to which star's *gradient energy* ∼ *potential energy*, the radius of the star, i.e. its core in which most of its energy is contained, can be estimated from

$$(\nabla\phi)^2 \sim V(\phi),$$
$$\frac{\sigma^2}{\tilde{R}^2} \sim \tilde{m}_\phi^2\sigma^2 + \lambda_\phi\sigma^4. \tag{31}$$

This then implies that the mass of a boson star scales as the radius, $\tilde{M} \propto \tilde{R}$, leading to

$$M \xrightarrow{\sim} \beta M. \tag{32}$$

For example, for a compact object whose radial size is $R \sim 10$ km $= \beta\,\bar{l}_P$, we obtain that $\beta$ is of the order of $\beta \sim 10^{38}$. It then follows that the mass of the scalar field changes from $m_\phi \sim \bar{m}_P$ to $m_\phi \sim 10^{-38}\bar{m}_P$ and the coupling constant from $\lambda_\phi \sim 1$ to $\lambda_\phi \sim 10^{-76}$. In the light of equation (20), the total mass from $M \sim \bar{m}_P$ changes to $M \sim 0.2\,M_\odot$, where $M_\odot = 2 \times 10^{30}$ kg is the solar mass.

On the other hand, one can start by setting the scalar field mass $m_\phi$ and estimate the resulting star radius and its total mass. This allows one to build models that can account for astrophysical objects of vastly different sizes, namely from dark compact objects [32, 33] to galactic dark matter halos [28, 29, 34].

## 3. Ordinary boson stars: case of minimal coupling

Since the properties of the boson stars with quartic self-interaction are quite extensively studied in [11], here we shall only briefly discuss their main characteristics. Perhaps the most peculiar feature of these configurations is the anisotropy in their principal pressures. Whereby in the (usual) fluid approach to compact stars, anisotropy is treated as a rather dubious and speculative concept (e.g. in the physics of neutron stars), it appears as a fairly natural property of boson stars. One can verify this by inspecting equations (10) and (11), which for $\xi = 0$ yield

$$\Pi = p_t - p_r = -2\mathrm{e}^{-\lambda}\phi_0'^2. \tag{33}$$

Here, we have identified the components of the energy–momentum tensor as

$$T_\mu^\nu = \mathrm{diag}(-\rho, p_r, p_t, p_t), \tag{34}$$

where $\rho$ is the energy density, $p_r$ the radial pressure and $p_t$ is the tangential pressure ($p_t = p_\theta = p_\phi$).

From equation (33), we see that anisotropy is strictly a negative function of the radial coordinate. This fact entails that, regardless of the coupling strength, for minimal coupling, one can only create configurations with $p_r \geqslant p_t$. In the following section, we elaborate more on the consequences of this fact.

In order to build a viable astrophysical object, its stability is clearly a basic requirement. Stability of boson stars has been extensively studied in the literature both analytically [35–37] and numerically [39, 40, 38] [3]. Numerical methods include dynamical evolution of the system at hand, whilst the analytical ones rely on the standard Chandrasekhar's methods, i.e. studying the response to a linear perturbation of *static* equilibrium configurations, whereby the total particle number is conserved [4]. Both avenues, however, lead to the same conclusion that can be summarized as follows. There exists a critical value of the central field $\sigma_c$ for which the

[3] The catastrophe theory is another interesting method that can be found in [41].

[4] Since the action (3) is invariant under the $U(1)$ symmetry, according to the Noether theorem, there is a conserved (scalar) charge density.

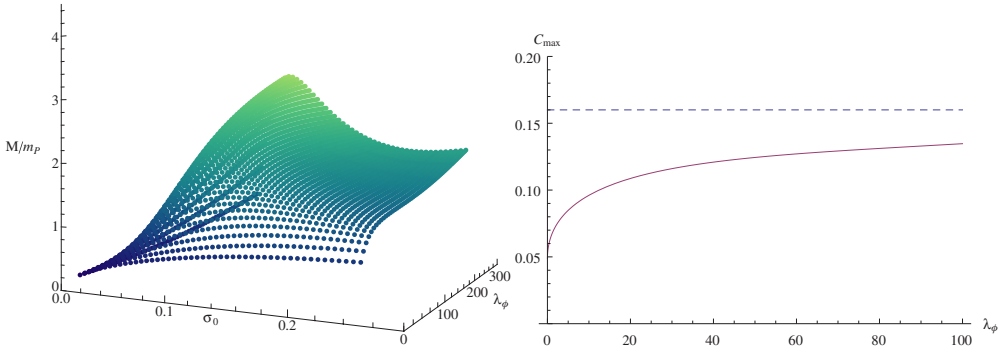


**Figure 1.** The star mass as a function of the central field value $\sigma_0$ and $\lambda_\phi$ for $\xi = 0$ in the left panel and the maximal effective compactness as a function of $\lambda_\phi$ in the right panel. Also $m_\phi^2 = \bar{m}_P^2$.

ground state of a boson star (nodeless in $\sigma(x)$) will be marginally stable upon small radial perturbations. For this critical field value, the total mass of the star exhibits turnaround in an $M(\sigma_0)$-curve (see e.g. [42]). Then, the configurations left from the peak are stable and those right from the peak are unstable leading to the collapse to a black hole or a dispersion at infinity. An interested reader may find a discussion in [43] on what is the likely fate of the boson star for the right-from-the-peak configurations in the $M(\sigma_0)$-curve. In the absence of the self-interaction, it was found that the maximally allowed mass is $M_{\max} = 0.633\, m^2_{\text{Planck}}/m_\phi$, and by switching on the self-interaction it increases as $M_{\max} = 0.22\sqrt{\Lambda}\, m_{\text{Planck}}/m_\phi$, where $\Lambda = \lambda_\phi(4\pi G_N m_\phi^2)$. In the left panel of figure 1, we show the star mass as a function of the central field values $\sigma_0$ and $\lambda_\phi$. As the amplitude $\sigma_0$ increases its mass also increases (while its radius decreases). For increasing $\lambda_\phi$, the maximum mass also increases, while the critical central field value $\sigma_c$ decreases.

Albeit self-interacting boson stars have been extensively studied in the literature, the explicit behaviour of their thermodynamic functions, i.e. of the energy density and the principal pressures, is lacking. Thereby, here we plot these (and other relevant) functions for two distinctive regimes: a vanishing self-interaction and a large self-interaction coupling constant. For any given value of the coupling constant, there is only one configuration that meets those of the maximally allowed mass. In figure 2, we show two such configurations for $\lambda_\phi = 0$ and $\lambda_\phi = 100$. In the left panel, the profiles of the scalar field and the metric functions (inset) are shown, while in the right panel we show the behaviour of the energy densities and the corresponding pressures (inset). Two main criteria can be read off from these graphs. The first is the interplay among the central field value and the radius: while one is increasing, the other one is decreasing and *vice versa*. An important consequence of this trend is the equivalence between the $M(\sigma_0)$ and the $M(R)$-curve. That is, both curves exhibit turnaround behaviour for equal maximally allowed masses, and hence either can be used for stability analysis. Second, the anisotropy in the principal pressures becomes less prominent due to the inclusion of self-interaction. This behaviour implies that boson stars built from strongly self-interacting fields tend to be more isotropic. Indeed, in this regime, boson stars behave like a polytrope with the EoS $p_t \approx p_r \propto \rho^{1+1/n}$, where $n$ is the polytropic index.

It is also worth noting here that the negative anisotropy (33) cannot rise to more exotic structures with negative principal pressures found in dark energy stars (e.g. gravastars). For the latter, one needs anisotropy to be a positive function of the radial coordinate (see e.g. [44, 6]). This is the main reason why we extend this analysis to include nonminimal coupling.

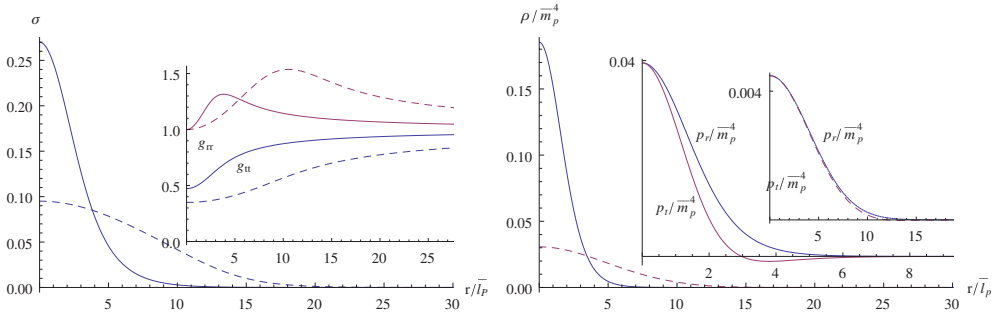


**Figure 2.** Left panel: the scalar field as a function of the radial coordinate and in the inset the metric functions $g_{tt}$ and $g_{rr}$. Right panel: the energy densities and the principal pressures in the inset. The solid curves are plotted for $\lambda_\phi = 0$ ($\{\sigma_c,\ M_{\max}\} = \{0.27,\ 0.633\,\bar{m}_P\}$) and the dashed curves are plotted for $\lambda_\phi = 100$ ($\{\sigma_c,\ M_{\max}\} = \{0.095,\ 2.257\,\bar{m}_P\}$). Also, $m_\phi^2 = \bar{m}_P^2$ and $\xi = 0$.

## 4. Dark energy-like stars: effects of nonminimal coupling

Spherically symmetric static configurations of a nonminimally coupled scalar field modelled by the action (3) in the absence of the quartic self-interaction were studied by Bij and Gleiser in [45]. Adopting the $M(\sigma_0)$ stability criterion, the authors calculated the critical (maximally allowed) mass and the critical particle number for a variety of values of the coupling constant $\xi$. The analysis is performed for boson stars both in the ground state (no nodes in the scalar field) and in excited states (higher nodes in the scalar field). However, the authors did not analyse the behaviour of the thermodynamic functions, namely of the energy density and pressures.

In the case of nonminimal coupling, the anisotropy becomes a rather convoluted function of matter *and* geometry:

$$\Pi = -2\mathrm{e}^{-\lambda}\phi_0'^2 - 2\xi\left(G_\theta^\theta - G_r^r\right)\phi_0^2 + 2\xi\mathrm{e}^{-\lambda}\left(\nu' + \frac{4}{r}\right)\phi_0\phi_0' - 4\xi\left(m_\phi^2 + \lambda_\phi\phi_0^2 - \omega^2\mathrm{e}^{-\nu} - \xi R\right)\phi_0^2. \tag{35}$$

As mentioned in the previous section, it is likely that equation (35) may become positive for some radii, which is an important ingredient of building microscopic configurations with negative pressures.

However, when dealing with spherically symmetric, localized, configurations of matter it seems reasonable to invoke the energy conditions as important criteria for physically acceptable matter.

### *4.1. Constraints from the energy conditions*

Various energy conditions have been proposed as reasonable physical restrictions on matter fields. They originate from the Raychaudhuri equation together with the requirement that gravity should be attractive (see e.g. [46, 47, 24]). When translated to the energy–momentum tensor for an anisotropic matter they read

$$\begin{aligned}
&\text{The weak energy condition (WEC)} && \rho \geqslant 0, \quad \rho + p_r \geqslant 0, \quad \rho + p_t \geqslant 0,\\
&\text{The dominant energy condition (DEC):} && \rho - p_r \geqslant 0, \quad \rho - p_t \geqslant 0,\\
&\text{The strong energy condition (SEC):} && \rho + p_r + 2p_t \geqslant 0.
\end{aligned} \tag{36}$$

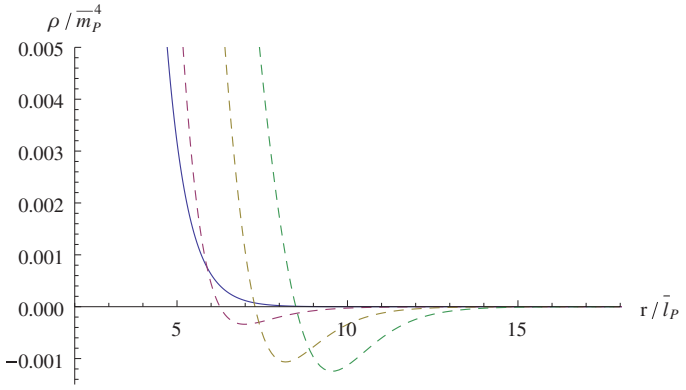


**Figure 3.** The energy density as a function of the radial coordinate. The solid curve stands for $\xi = \xi_{\text{crit}}^{\text{WEC}} = -1$, the dashed curves are for $\xi = -2, -4, -6$ from left to right, respectively. Also, $\lambda_\phi = 0$ and $m_\phi^2 = \bar{m}_P^2$.

The WEC imposes the requirement of a positive energy density measured by any observer. Also, the energy density plus pressures in any direction needs to be positive. The DEC requires that the pressures of the fluid do not exceed the energy density, so that the local sound speed in any observable fluid is always less than the speed of light in vacuum. The SEC has very interesting implications. Its violation lead to regions of repulsive gravity such as in cosmological inflation and gravastars. Hence, it is reasonable to require that the WEC and DEC are satisfied by a fluid, but that the SEC may be violated.

With or without self-interaction it turns out that the WEC is obeyed for nonminimal couplings only *if* greater than a certain (negative) critical value $\xi > \xi_{\text{crit}}^{\text{WEC}}$, whereby $\xi_{\text{crit}}^{\text{WEC}}$ decreases very slowly as $\lambda_\phi$ increases. As an example of the indicated transition, we plot the energy density in figure 3 where it is shown that the violation of the WEC is more prominent as the value of the nonminimal coupling decreases.

One example of a spacetime that violates the WEC is that of a wormhole (see e.g. [48–51]). Some other examples would include a more exotic matter. Although this energy condition is also violated by certain quantum fields, a positive energy density is an essential feature of the classical forms of matter. A consequence of the requirement that the WEC is satisfied is a shift in the 'maximally' allowed masses to lower values as depicted in figure 4 for $\xi < \xi_{\text{crit}}^{\text{WEC}}$.

In addition, we also require that the energy is not transported faster than light, and hence the DEC should be satisfied. Another constraint on parameter space emerges from the requirement $\xi > \xi_{\text{crit}}^{\text{DEC}}$ as shown in figure 4. The dashed curves represent the maximally allowed masses for the by-the-WEC-and-DEC modified configurations, while the solid curves correspond to the old (non-modified) configurations. As such, figure 4 represents an important result of this paper due to the fact that it establishes new configurations for stars that satisfy the WEC and DEC.

The SEC is also violated for certain nonminimal couplings, $\xi > \xi_{\text{crit}}^{\text{SEC}}$. As opposed to the problem of violating the WEC and DEC, a violation of the SEC is actually favourable in building highly compact objects. Namely, a region of a compact object that violates the SEC exhibits repulsive gravity, which is desirable. Violation of the SEC plays an important role in the early universe cosmology, where it is used to explain the origin of Universe's large-scale structure generated through matter and gravitational perturbations amplified during a hypothetical inflationary epoch in which the SEC is violated. It is also an essential component

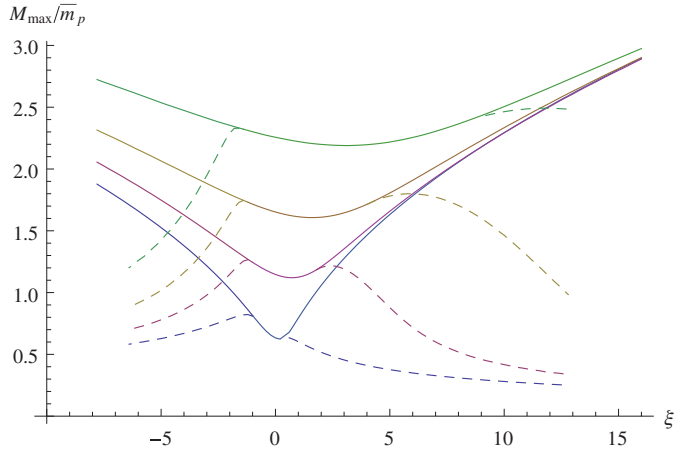


**Figure 4.** The maximum mass as a function of the coupling $\xi$ for $\lambda_\phi = \{0, 20, 50, 100\}$ from bottom to top. Also, $m_\phi^2 = \bar{m}_P^2$. For $\xi < 0$, the dashed curves describe configurations that obey the WEC and for $\xi > 0$ configurations that obey the DEC. The solid curves describe configurations that are not constrained by energy conditions.

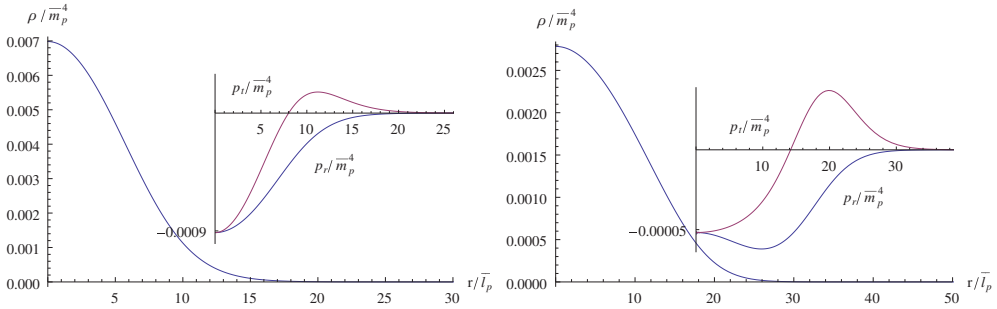


**Figure 5.** The energy density and the principal pressures (insets) for $m_\phi^2 = \bar{m}_P^2$, $\xi = -4$ and for (*a*) $\{\lambda_\phi, \sigma_c\} = \{0, 0.050\}$ in the left panel and (*b*) $\{\lambda_\phi, \sigma_c\} = \{100, 0.034\}$ in the right panel.

of gravastars, which in their interior, where $p_r(0) = p_t(0) = -\rho(0)$, strongly violate the SEC. In the case of gravastars, violation of the SEC is crucial for large values of compactness. Unfortunately, here the SEC is significantly violated only if the DEC is violated. Nevertheless, we shall explore some effects of violating the SEC in the following subsection.

### *4.2. Energy density and pressures profiles*

It is now of interest to explore thermodynamic functions, namely the energy density and the principal pressures.

Depending on the strength of the self-interaction, configurations with negative principal pressures emerge that can be described by the EoS $p_r \propto -\rho^\beta$. This particular EoS is used to describe *dark energy stars*. Even though these configurations exhibit negative principal pressures, the SEC is not violated thus excluding regions with repulsive gravity.

One such configuration is shown in the left panel of figure 5. As a matter of fact, in the absence of self-interaction, for $\xi < \xi_{\mathrm{crit}}^{\mathrm{WEC}}$ all configurations lying on the $M_{\max}(\xi)$-curve can

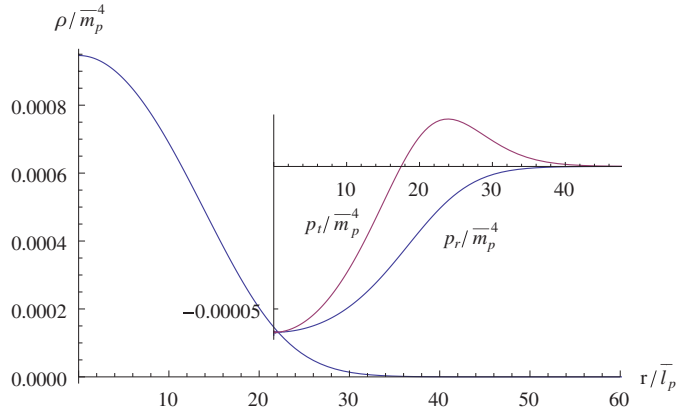


**Figure 6.** The energy density and the principal pressures (inset) for $\xi = -8$, $\lambda_\phi = 100$, $\sigma_c = 0.02$. Also $m_\phi^2 = \bar{m}_P^2$.

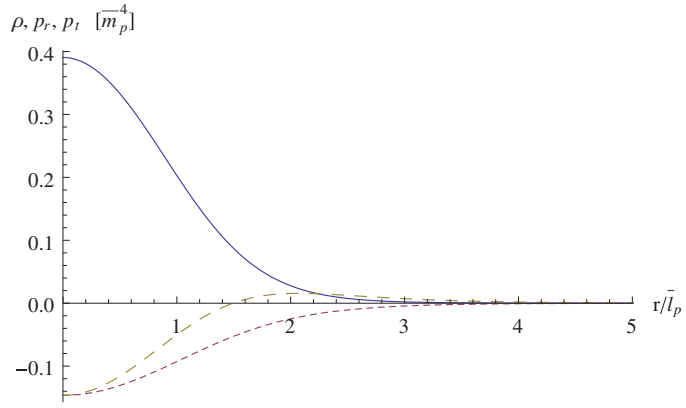


**Figure 7.** The energy density (solid curve), radial (short-dashed curve) and transversal pressure (long-dashed curve) for $\xi = -0.9$, $\lambda_\phi = -30$, $\sigma_0 = 0.26$. Also $m_\phi^2 = \bar{m}_P^2$.

be described by the EoS of a dark energy star, $p_r \propto -\rho^\beta$. When the self-interaction increases, the pressures increase as well, as can be seen in the right panel of figure 5. Nevertheless, no matter how large the self-interaction is, the dark energy star-like configurations are obtained by choosing an appropriate (i.e. negative enough) nonminimal coupling. This effect is clearly shown by comparing figure 6 with figure 5. It is also of interest to observe that the transversal pressures of these configurations, as positive near surface, are like those of gravastars. This fact brings us to the idea that the gravastars, as not yet formulated within the field theories and as such still of interest to explore, might be produced in modified gravity that includes higher order terms in the Ricci scalar, Ricci tensor and/or Riemann curvature tensor.

However, proper dark energy stars, i.e. with negative pressures and violating SEC, can be obtained for $\lambda_\phi < 0$. We present one such solution in figure 7. It is interesting that this solution violates only the SEC, while the weak and dominant energy conditions are obeyed. Nevertheless, theories with negative potentials yield Hamiltonians that are unbounded from below, and are at best quasi-stable, i.e. field configurations will eventually 'decay' into large fields and roll down to infinity, where energy is minus infinity (see e.g. [29]).

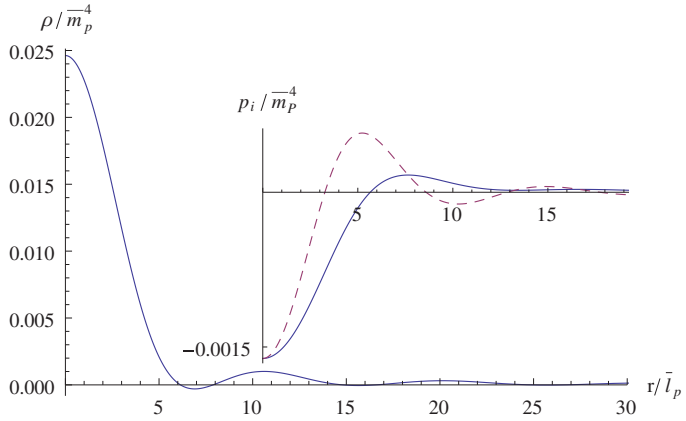


**Figure 8.** The energy density, radial (solid curve in the inset) and transversal pressure (dashed curve in the inset) for $\xi = -0.7$, $\lambda_\phi = 0$, $\sigma_0 = 0.1$ and $m_\phi^2 = 0.9\,\bar{m}_P^2$.

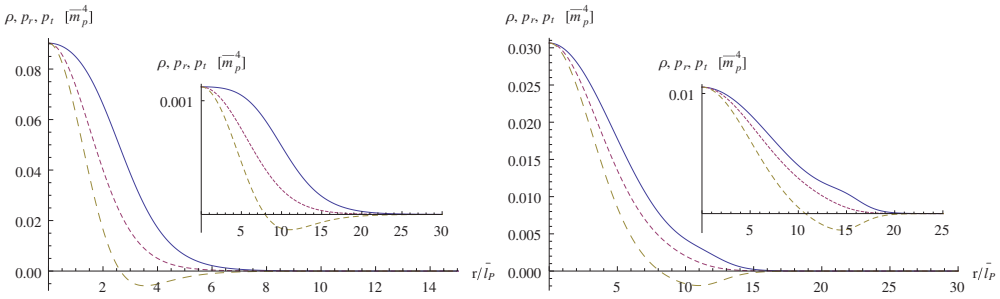


**Figure 9.** The energy density (solid), the radial pressure (short-dashed) and the transversal pressure (long-dashed) for (*a*) left panel: $\lambda_\phi = 0$ and $\{\xi, \sigma_c\} = \{0.6, 0.2635\}$ and in the inset $\{6.4, 0.0364\}$ and (*b*) right panel: $\lambda_\phi = 100$ and $\{\xi, \sigma_c\} = \{7.8, 0.1194\}$ and in the inset $\{12.8, 0.0845\}$. Also $m_\phi^2 = \bar{m}_P^2$.

When the excited states of these configurations are considered, the energy density and pressures oscillate in space. Both pressures are now positive functions of coordinate in the region near the surface thus resembling gravastars solutions. We show one such configuration in figure 8. However, even though stability might not be questionable in this setting, the weak and dominant energy conditions are violated. Yet, it was argued in [29] that a galactic halo consisting of highly excited states of ordinary boson stars could explain the rotation of low-luminosity spiral galaxies.

Configurations obtained for positive values of nonminimal coupling exhibit positive pressures and hence are quite similar to the ordinary boson stars. In figure 9, we plot the energy density, radial and transversal pressure for $\lambda_\phi = 0$ in the left panel and $\lambda_\phi = 100$ in the right panel. For each $\lambda_\phi$, two configurations are presented, one for $\xi_{\text{crit}}^{\text{DEC}}$ and the other one for a nonminimal coupling that is much larger than the critical one. For each $\lambda_\phi$, the effect of increasing $\xi$ is only to decrease mass and increase the radius (thus decreasing the compactness) without any drastic changes in the behaviour of energy density and pressures. However, the profiles of the energy density and pressures qualitatively do change considerably for different $\lambda_\phi$. In the right panel of figure 9, the hump in the energy density occurs as $\xi$ increases. This

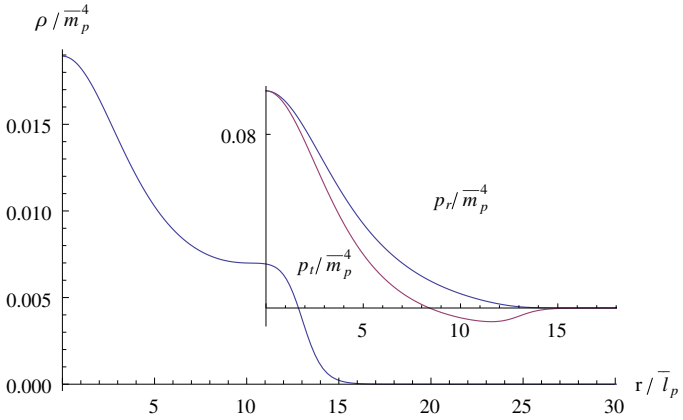


**Figure 10.** The energy density and the principal pressures (insets) for $m_\phi^2 = \bar{m}_P^2$, $\xi = 16$, $\{\lambda_\phi, \sigma_c\} = \{0, 0.145\}$.

hump is actually followed by a violation of the SEC which is more significant for larger $\xi$. Hence, the hump in the inset of figure 9 is more prominent. In order to justify this statement in figure 10, we plot the energy density and pressures for a configuration that strongly violates the SEC (in the region of negative transversal pressure—see the inset in figure 10).

In this subsection, we have seen that static, equilibrium configurations of the self-interacting scalars may exist even though the radial pressure does not exhibit locally positive values. This feature of boson stars is to be contrasted with the stars made of fermionic gas (for which the pressures must be positive and as such help balance matter against gravitational collapse). This ambiguity is clarified if we realize that the (radial) pressure must be positive only if we deal with the fluids, which are obtained as highly excited states of the bosonic or fermionic fields. In the case of the boson stars made of the ground state scalar field configurations, a static, equilibrium solution is obtained only for *charged* fields (i.e. there are no stable (gravitationally bounded) solutions for the real scalar fields), that is, a scalar charge stabilizes the boson star.

Apart from the qualitative behaviour of the energy density and pressures, from this subsection one could also infer subtle relations among the total masses and radii. In particular, increasing the central field value is followed by a decreasing radius up to the maximally allowed mass. This interplay among the mass and the radius is best explored by analysing the effective compactness.

### *4.3. Effective compactness*

Following [52], we define the *effective compactness* as

$$C(\sigma_0, \lambda_\phi) = \frac{M_{99}(\sigma_0, \lambda_\phi)}{R_{99}}, \tag{37}$$

where $R_{99}$ is the radius at which the mass, defined in terms of the metric function $e^{-\lambda} = 1 - 2m/r$, equals 99% of the total mass $M = m(\infty)$. The effective radius owes this sort of definition as the scalar field is (exponentially) infinitely extended and thus always with zero compactness.

As shown in [52] the effective compactness in a minimal setting increases with the self-coupling $\lambda_\phi$ and as $\lambda_\phi \to \infty$ the maximal effective compactness approaches $C_{\max} \approx 0.16$ as

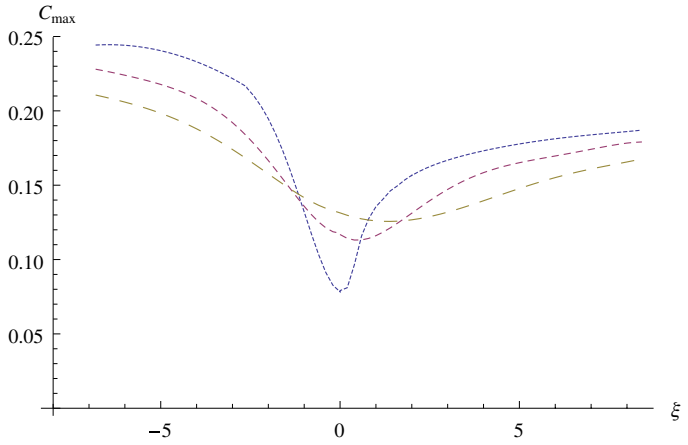


**Figure 11.** The effective compactness as a function of the $\xi$-coupling for $\lambda_\phi = 0$ (dotted curve), $\lambda_\phi = 20$ (short dashed curve) and $\lambda_\phi = 50$ (long dashed curve). Also $m_\phi^2 = \bar{m}_P^2$.

shown in the right panel of figure 1. For each $\lambda_\phi$, the maximal compactness corresponds to the parameters matching the critical field value $\sigma_c$. That is the maximally allowed mass and its radius.

If $M_{\max}$ is not constrained by the weak and dominant energy conditions, then the effective compactness for $\xi > 0$ is largest for large $\xi$ and $\lambda_\phi = 0$ as shown in figure 11 and approaches $C_{\max} \approx 0.20$. This value is only slightly larger than the maximal effective compactness obtained in the minimal setting and can be related to an SEC violation. Why this value is not larger, probably can be explained with the fact that the SEC is violated only near the surface where the transversal pressures become negative.

However, for $\xi < 0$ the compactness is much greater and reaches its maximum value for large negative values of the nonminimal coupling and also in the case when $\lambda_\phi = 0$, which approximately equals $C_{\max} \gtrsim 0.25$. Even though the SE is not violated in this region, an increased effective compactness can be attributed to negative pressures that weaken gravity, thus enabling more matter to be accommodated in a fixed volume. This result is also very important as it suggests that, in order to build a highly compact object, we ought to have configurations with negative principal pressures *and* a violation of the SEC.

When restrictions from the weak and dominant energy conditions are included, the effective compactness behaves as shown in figure 12. The maximal values for each $\lambda_\phi$ are obtained for $\xi_{\text{crit}}^{\text{WEC,DEC}}$ and then abruptly decrease with increasing/decreasing nonminimal coupling. This brings us to the conclusion that the most compact objects are produced in the domain of negative pressures and large self-couplings, with the maximum effective compactness only slightly larger than the minimal case $C_{\max} \gtrsim 0.16$.

Nevertheless, figures 11 and 12 are very useful, as one can easily relate the mass to the radius. If we want to create a compact object with, for example, a radius of $R = 15\,\text{km}$, then from $C_{\max}$ one can easily read off its mass. The range of effective compactness $C_{\max} = 0.05 - 0.25$ correspond to the masses $M = (0.5 - 2.5)\,M_\odot$.

However, in order to obtain scalar's masses and self-couplings, one needs to employ the universality described in section 2. By fixing the radius to, e.g., $R = 15\,\text{km}$, one can calculate $\beta$ for any configuration with differing radii (in the reduced Planck units). Then, the scalar's mass and self-coupling are easily obtained by applying the rescaling conditions $m_\phi^2 \to m_\phi^2/\beta^2$ and $\lambda_\phi \to \lambda_\phi/\beta^2$. By inspection of all above diagrams depicting the energy

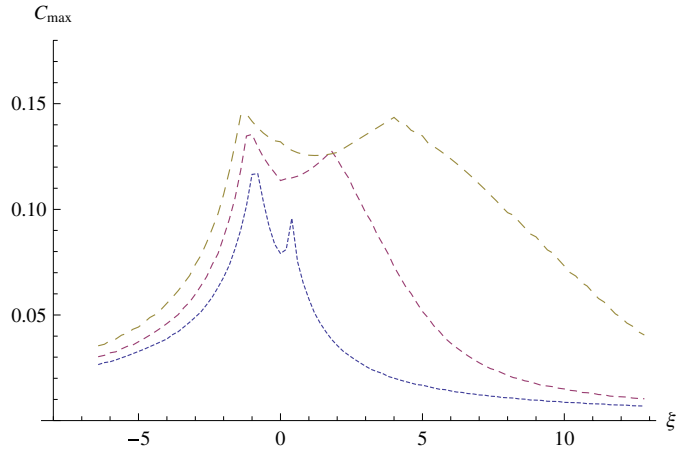


**Figure 12.** The effective compactness as a function of $\xi$ for configurations that obey the WEC and DEC. $\lambda_\phi = 0$ (dotted curve), $\lambda_\phi = 20$ (short dashed curve) and $\lambda_\phi = 50$ (long dashed curve). Also $m_\phi^2 = \bar{m}_P^2$.

density and pressures (in previous subsection), it can be inferred that the radii of all given configurations roughly fall within the range $r = (10 - 40)\,\bar{l}_P$. Hence, if we want to create a star of $R = 15\,\text{km}$ the corresponding $\beta$s are $\beta = (18.6 - 4.6) \times 10^{36}$ leading to the scalar's masses $m_\phi = (0.27 - 1.08) \times 10^{-8}\,\text{eV}$, which could be in the range of the neutrino masses. To calculate the rescaled self-coupling, let us, for convenience, take its starting value $\lambda_\phi = 50$. After the rescaling we obtain $\lambda_\phi = (14 - 0.24) \times 10^{-73}$. But of course, if one considers a case when the coupling has reached saturation, one could increase the value of the unrescaled $\lambda_\phi$ arbitrarily, which would then yield more reasonable (i.e. larger) values of the rescaled $\lambda_\phi$.

## 5. Conclusions

In this paper, we have examined spherically symmetric configurations made of a scalar field nonminimally coupled to gravity. Our results are in perfect agreement with those of Colpi and collaborators [11] for self-interacting minimally coupled scalars and with those of Bij and Gleiser [45] for a non-self-interacting, nonminimally coupled scalar field.

We have shown that already a *minimal* extension of Einstein's theory to the nonminimal coupling results in radically different configurations from standard boson stars, i.e. dark energy-like stars which are characterized by negative principal pressures. Upon investigating the energy conditions in more detail, it turned out that the strong energy condition (SEC), which should be violated in the interior of dark energy stars, and whose violation signals repulsive gravity, is satisfied in the interior of these configurations. However, we presented an example of a *proper* dark energy star, i.e. with negative pressures and a violating SEC, which is obtained for a negative self-interaction. Even though the configuration presented here does not suffer from violation of the weak and dominant energy condition, configurations with negative potentials, in general, are not that appealing due to their stability issues. We also presented one higher mode solution that led to gravastar-like principal pressures. That is, both principal pressures reveal positive atmosphere (region near surface). But, the SEC is obeyed, while the weak and dominant conditions are violated, thus again without spacetime regions with repulsive gravity.

When imposing restrictions on classical matter by energy conditions we found regions of parameter space for which both the weak and dominant energy conditions are violated. In particular, the weak energy condition (WEC) is violated for all negative values of the nonminimal coupling, if it is less than a critical value $\xi < \xi_{\rm crit}^{\rm WEC}$. The dominant energy condition (DEC) is violated for all positive values of the nonminimal coupling if greater than a critical value $\xi > \xi_{\rm crit}^{\rm DEC}$. The consequences of a violation of the WEC and DEC are encoded in the maximally allowed masses that are now shifted to lower values. The SEC is violated in the region of a positive nonminimal coupling and is followed by humps in the energy density. Even though the violation of the energy conditions does not support the view of classical matter, it would be of interest to explore in more detail the imprint of a test particle moving in such a background.

Furthermore, we analysed the effective compactness for configurations that do or do not satisfy the WEC and DEC, and found that the maximum effective compactness is attained in the regimes of negative pressures for non-self-interacting configurations and equals $C_{\rm max} \gtrsim 0.25$ for configurations that violate the WEC and $C_{\rm max} \gtrsim 0.16$ for those configurations that obey the WEC and DEC. This result sets limits on the boson star mass. For example, when $R = 15\,{\rm km}$ the maximum mass is $M = (2 - 2.5)\,M_{\odot}$ which belongs in the domain of neutron stars. Even though the SEC is not violated, an increased maximum effective compactness could be related to the existence of negative pressures.

In addition, we developed a universality condition based upon which one can calculate scalar's masses and self-couplings for all given configurations. Even though in this paper we focused on parameters that yield compact objects, with the universality condition it is possible to extend this analysis to larger structures that match galactic sizes, such as, for example, dark matter halos. An investigation of observational constraints on the model are underway.

Although theories with a nonminimally coupled scalar field represent a simple and quite benign extension of general relativity, they provide a plethora of different interesting astrophysical structures, ranging from isotropic polytropes to highly anisotropic dark energy-like stars. Nevertheless, within this model it is, in fact, not possible to create a *highly* compact, nonsingular object whose characteristics are arbitrarily close to those of the Schwarzschild black hole. Yet, from this work one can infer that the real black hole mimicker might be produced in the context of modified theories of gravity.

## Acknowledgments

AM would like to thank Tomislav Prokopec for careful reading of the manuscript and for useful suggestions. This work is partially supported by the Croatian Ministry of Science under the project no. 036-0982930-3144 and also by the CompStar—Research Networking Programme of the European Science Foundation.

## References

[1] Sakharov A D 1966 *Sov. Phys.—JETP* **22** 241
[2] Gliner E B 1966 *Sov. Phys.—JETP* **22** 378
[3] Mazur P O and Mottola E 2004 Gravitational condensate stars: an alternative to black holes *Proc. Natl Acad. Sci.* **101** 9545 (arXiv:gr-qc/0109035)
[4] Visser M and Wiltshire D L 2004 Stable gravastars—an alternative to black holes? *Class. Quantum Grav.* **21** 1135 (arXiv:gr-qc/0310107)
[5] Martin-Moruno P, Garcia N M, Lobo F S N and Visser M 2012 Generic thin-shell gravastars *J. Cosmol. Astropart. Phys.* JCAP03(2012)034 (arXiv:gr-qc/1112.5253)
[6] DeBenedictis A, Horvat D, Ilijić S, Kloster S and Viswanathan K S 2006 Gravastar solutions with continuous pressures and equation of state *Class. Quantum Grav.* **23** 2303 (arXiv:gr-qc/0511097)

[7] Horvat D, Ilijić S and Marunović A 2009 Electrically charged gravastar configurations *Class. Quantum Grav.* **26** 025003 (arXiv:gr-qc/0807.2051)

[8] Horvat D, Ilijić S and Marunović A 2011 Radial stability analysis of the continuous pressure gravastar *Class. Quantum Grav.* **28** 195008 (arXiv:gr-qc/1104.3537)

[9] Kaup D J 1968 Klein–Gordon geon *Phys. Rev.* **172** 1331–42

[10] Ruffini R and Bonazzola S 1969 Systems of self-gravitating particles in general relativity and the concept of an equation of state *Phys. Rev.* **187** 1767

[11] Colpi M, Shapiro S L and Wasserman I 1986 Boson stars: gravitational equilibria of self-interacting scalar fields *Phys. Rev. Lett.* **57** 2485

[12] Friedberg R and Lee T D 1977 *Phys. Rev.* D **16** 1096

[13] Lee T D and Pang Y 1992 *Phys. Rep.* **221** 251

[14] Jetzer P and van der Bij J J 1989 Charged boson stars *Phys. Lett.* B **227** 341–6

[15] Seidel E and Suen W-M 1991 Oscillating soliton stars *Phys. Rev. Lett.* **66** 1659–62

[16] Liebling S L and Palenzuela C 2012 Dynamical boson stars *Living Rev. Rel.* **15** 6

[17] Schunck F E and Mielke E W 2003 General relativistic boson stars *Class. Quantum Grav.* **20** R301–56

[18] Jetzer P 1992 Boson stars *Phys. Rep.* **220** 163–227

[19] Liddle A R and Madsen M S 1992 The structure and formation of boson stars *Int. J. Mod. Phys.* D **1** 101–43

[20] Dymnikova I 1992 Vacuum nonsingular black hole *Gen. Rel. Grav.* **24** 235–42

[21] Dymnikova I and Galaktionov E 2005 Stability of a vacuum nonsingular black hole *Class. Quantum Grav.* **22** 2331–58 (arXiv:gr-qc/0409049)

[22] Lobo F S N 2006 Stable dark energy stars *Class. Quantum Grav.* **23** 1525–41 (arXiv:gr-qc/0508115)

[23] Ghezzi C R 2011 Anisotropic dark energy stars *Astrophys. Space Sci.* **333** 437–47 (arXiv:gr-qc/0908.0779)

[24] Rahaman F, Yadav A K, Ray S, Maulick R and Sharma R 2011 Singularity-free dark energy star *Gen. Rel. Grav.* (arXiv:gr-qc/1102.1382) at press

[25] Yazadjiev S S 2011 Exact dark energy star solution *Phys. Rev.* D **83** 127501 (arXiv:gr-qc/1104.1865)

[26] Derrick G H 1964 Comments on nonlinear wave equations as models for elementary particles *J. Math. Phys.* **5** 1252–4

[27] Jetzer P and Scialom D 1997 On the stability of real scalar boson stars arXiv:gr-qc/9709056

[28] Arbey A, Lesgourges J and Salati P 2003 Galactic halos of fluid dark matter *Phys. Rev.* D **68** 023511 (arXiv:astro-ph/0301533)

[29] Arbey A, Lesgourges J and Salati P 2001 Quintessential halos around galaxies *Phys. Rev.* D **64** 123528

[30] Bernal A, Barranco J, Alic D and Palenzuela C 2010 Multistate boson stars *Phys. Rev.* D **81** 044031

[31] Ascher U, Christianse J and Russell R D 1978 COLSYS: Collocation software for boundary value ODE's (www.netlib.org/ode/colsys.f)

[32] Hernandez X, Matos T, Sussman R A and Verbin Y 2004 Scalar field 'mini-mCHOs': a new explanation for galactic dark matter *Phys. Rev.* D **70** 043357

[33] Barranco J and Bernal A 2011 Self-gravitating system made of axions *Phys. Rev.* D **83** 043525

[34] Arbey A, Lesgourges J and Salati P 2002 Cosmological constraints on quintessential halos *Phys. Rev.* D **65** 083514

[35] Gleiser M and Watkins R 1989 Gravitational stability of scalar matter *Nucl. Phys.* B **319** 733–46

[36] Lee T D and Pang Y 1989 Stability of mini-boson stars *Nucl. Phys.* B **315** 477–516

[37] Jetzer P 1989 Stability of charged boson stars *Phys. Lett.* B **231** 433–8

[38] Seidel E and Suen W 1990 Dynamical evolution of boson stars: perturbing the ground state *Phys. Rev.* D **42** 384–403

[39] Hawley S H and Choptuik M W 2000 Boson stars driven to the brink of black hole formation *Phys. Rev.* D **62** 104024

[40] Guzman F S 2004 Evolving spherical boson stars on a 3D cartesian grid *Phys. Rev.* D **70** 044033

[41] Kusmartsev F V, Mielke E W and Schunck F E 1991 Gravitational stability of boson stars *Phys. Rev.* D **43** 3895–901

[42] Misner C W, Thorne K S and Wheeler J A 1973 *Gravitation* (San Francisco, CA: Freeman)

[43] Guzman F S 2009 The three dynamical fates of boson stars *Rev. Mex. Fis.* **55** 321–6

[44] Cattoen C, Faber T and Visser M 2005 Gravastars must have anisotropic pressures *Class. Quantum Grav.* **22** 4189 (arXiv:gr-qc/0505137)

[45] van der Bij J J and Gleiser M 1987 Stars of bosons with non-minimal energy–momentum tensor *Phys. Lett.* B **194** 482

[46] Carroll S 2004 *Spacetime and Geometry: An Introduction to General Relativity* (New York: Addison-Wesley)

[47] Horvat D and Ilijić S 2007 Gravastar energy conditions revisited *Class. Quantum Grav.* **24** 5637–49 (arXiv:gr-qc/0707.1636)

[48] DeBenedictis A and Horvat D 2012 On wormhole throats in $f(R)$ gravity theory *Gen. Rel. Grav.* **44** 2711–44

[49] Visser Matt 1995 *Lorentzian Wormholes: from Einstein to Hawking* (New York: AIP)
[50] Barcelo C and Visser M 2000 Scalar fields, energy conditions and traversable wormholes *Class. Quantum Grav.* **17** 3843 (arXiv:gr-qc/0003025)
[51] Lobo F 2008 Exotic solutions in general relativity: traversable wormholes and 'warp drive' spacetimes *Classical and Quantum Gravity Research* (Hauppauge, NY: Nova Science) pp 1–78 ISBN 978-1-60456-366-5 (arXiv:0710.4474)
[52] Amaro-Seoanea P, Barrancoa J, Bernala A and Rezzolla L 2010 Constraining scalar fields with stellar kinematics and collisional dark matter *J. Cosmol. Astropart. Phys.* JCAP11(2010)002